Applied Catalysis B: Environmental 110 (2011) 171–177

Contents lists available at SciVerse ScienceDirect

Applied Catalysis B: Environmental

journal homepage: www.elsevier.com/locate/apcatb

In situ FT-IR investigation on the selective catalytic reduction of NO with CH_4 over Pd/sulfated alumina catalyst

Hongyan Zhang[a,b], Lin Li[a], Ning Li[a], Aiqin Wang[a], Xiaodong Wang[a], Tao Zhang[a,*]

[a] State Key Laboratory of Catalysis, Dalian Institute of Chemical Physics, Chinese Academy of Sciences, Dalian, 116023, PR China
[b] Graduate University of Chinese Academy of Sciences, Beijing, 100049, PR China

ARTICLE INFO

Article history:
Received 25 October 2010
Received in revised form 30 July 2011
Accepted 31 August 2011
Available online 7 September 2011

Keywords:
Adsorption
$NO–O_2$ co-adsorption
In situ FT-IR
Nitrates
$deNO_x$
CH_4
SCR
Pd

ABSTRACT

In situ Fourier Transform Infrared (FT-IR) spectroscopy was applied to study the mechanism of the selective catalytic reduction (SCR) of NO with methane over 0.1 wt% Pd/sulfated alumina (SA) catalyst. Here, CO adsorption, NO adsorption, $NO–O_2$ co-adsorption and interaction of the intermediates after $NO–O_2$ adsorption with methane or methane/oxygen were investigated. The FT-IR results show that the Pd supported on Al_2O_3 mainly exists as oxide, such as PdO cluster. While, the Pd supported on SA mainly exists as isolated Pd^{2+} ions. The addition of Pd can promote the formation of nitro/nitrito and nitrate species on Al_2O_3 or SA at room temperature. At the same time, Pd also promotes the nitrates decomposition at high temperatures. Support sulfation further decreases the total concentration of the nitrates adsorbed on the surface of catalysts and lowers their thermal stability. Moreover, support sulfation can also stabilize isolated Pd^{2+} ions, which could catalyze the reaction between nitrate species and methane. Upon co-adsorption of NO and O_2 on 0.1 wt% Pd/SA catalyst, the intermediate Pd^{2+}–NO was produced. This intermediate could readily react with CH_4 and O_2, but almost not react with CH_4 over 350 °C.

1. Introduction

Selective catalytic reduction of NO with methane (CH_4-SCR) under lean-burn conditions has attracted a great deal of attention during the past decades [1–8]. So far, only limited types of metals, such as Co [9–11], Mn [12,13], Ni [14], In [15–18], Ga [19], and Pd [20], have been reported as active components for the CH_4-SCR reaction. Acidic support is necessary to maintain the metal components as highly dispersed cations. While the oxides of these metals, such as Co_3O_4, Mn_3O_4, PdO, are very active for the combustion of methane by oxygen [21–28]. Zeolites, possessing strong acid sites as well as ion-exchange capabilities, are the best supports for these metals used in CH_4-SCR reaction [29]. However, the serious poisoning effect of water vapor and sulfur dioxide in the exhaust limits significantly their industrial applications [30,31]. To solve this problem, metals supported on superacids such as sulfated TiO_2 (ST) and ZrO_2 (SZ), tungstated ZrO_2 (WZ) and Al_2O_3 (WA), have been developed in recent years [32–40].

Resasco and co-workers [28] reported that Pd/SZ was effective for CH_4-SCR reaction. In the following studies by other research groups, Pd/WZ and Pd/WA [38,41] catalysts were reported to have resistance to H_2O. Pd/Co-SZ [33,34] and In/ST [32] catalysts exhibited good resistance to H_2O and SO_2. Our group has found that Co/SZ [23], Mn/SZ [25], and Pd/SA [39] are excellent catalysts for the selective catalytic reduction of NO with methane under lean-burn conditions. Over theses catalysts, good catalytic performances were observed even in the presence of water vapor and SO_2. Sulfation of the support was found to suppress the combustion of methane and promote the reaction between NO_x species and CH_4. To understand this behavior, a variety of characterization techniques were employed to reveal the change of structure and state of active metals by the support sulfation. For example, for the Co/SZ catalyst, we found that sulfation of the support promoted the dispersion of Co species by stabilizing the Co^{2+} and preventing the formation of Co_3O_4 which favors the complete oxidation of CH_4 [23]. Kantcheva and Vakkasoglu [42,43] investigated NO_x species formed by NO adsorption and $NO–O_2$ co-adsorption on Co/SZ catalyst. They found that the nitro-nitrato species on the sulfated catalyst have a lower thermal stability than the nitrates on the unsulfated catalyst. They also studied the reactivity of nitro-nitrato species towards methane. Based on the results, they proposed that formate species and formic acid formed by CH_4 activation on Co sites are the key intermediates to reduce nitro-nitrato species [43]. In our previous work, we found the Pd/SA is a good catalyst for the selective reduction of NO with methane [39]. Compared with Co/SZ catalyst, Pd/SA is more active. However, to our knowledge, there is

* Corresponding author. Tel.: +86 411 84379015; fax: +86 411 84691570.
E-mail address: taozhang@dicp.ac.cn (T. Zhang).

0926-3373/$ – see front matter © 2011 Elsevier B.V. All rights reserved.
doi:10.1016/j.apcatb.2011.08.040

no report about FT-IR characterization for the selective catalytic reduction of NO with methane over Pd/SA catalyst. In this contribution, we employed in situ FT-IR spectroscopy to study the adsorbed NO_x species on 0.1 wt% Pd/SA catalyst and their reactivity towards methane or methane/oxygen mixture. Based on the spectra results, a reaction mechanism has been proposed for the CH_4-SCR of NO reaction.

2. Experimental

2.1. Preparation of catalysts

The γ-Al_2O_3 is home-made and has a BET surface area of 172 m^2/g. The sulfation of the support was accomplished by impregnation with 2.5 M H_2SO_4 in a ratio of 15 mL/g_{cat}, as described in our previous paper [39]. Pd was loaded on the support by incipient wetness impregnation with $PdCl_2$ as the precursor. All the samples including γ-Al_2O_3, 0.1 wt% Pd/γ-Al_2O_3, SA and 0.1 wt% Pd/SA were dried at 100 °C for 8 h and calcined in air at 600 °C for 6 h.

2.2. N_2 physisorption measurements

The specific BET surface areas were determined by nitrogen adsorption at 77 K using an ASAP 2010 apparatus. Before each measurement, the samples were evacuated at 350 °C for 3 h.

2.3. Temperature-programmed desorption measurements (TPD)

NO-TPD measurements were performed on a fixed-bed flow reactor connected with a mass spectrometer. Before the experiment, the sample (300 mg) was placed in a quartz reactor which was heated linearly with a rate of 10 °C/min up to 600 °C in He for 1 h, then cooled to room temperature. Adsorption of NO was carried out by passing 1% NO/He with the flow rate of 50 mL/min for 1 h, followed by purging with He for 30 min. The temperature of sample was elevated at a rate of 15 °C/min from room temperature to 600 °C under He flow. The desorbed NO was detected with mass spectrometer.

2.4. In situ FT-IR characterization

FT-IR measurements were performed on a Bruker spectrometer (EQUINOX55) equipped with DTGS detector at a spectral resolution of 4 cm^{-1} and accumulation of 120 scans.

Prior to the adsorption measurements, the samples were pressed into self-supporting pellets, and then treated in situ in the IR cell which was connected to a vacuum apparatus. Before the experiment, samples were activated by heating in oxygen at 500 °C for 30 min, evacuated at the same temperature for 1 h, and then cooled to room temperature. At this stage, the spectrum was recorded as the background reference. Subsequently, doses of NO, O_2, or CH_4 were introduced into the cell for adsorption. All the spectra were collected at room temperature, and presented here by subtracting the spectrum of the corresponding background reference.

The diffuse reflectance infrared Fourier transform spectroscopy (DRIFTS) spectra were also recorded on a Bruker spectrometer (EQUINOX55) equipped with MCT detector at a spectral resolution of 4 cm^{-1} and accumulation of 120 scans. The samples were finely ground, placed in a ceramic crucible. Prior to analysis, all samples were treated with oxygen at 500 °C for 30 min. The total flow rate of the feed gas was 100 mL/min. The background spectra were collected at the given temperature (350 °C) under He atmosphere for 30 min.

Table 1
Specific BET surface areas of the investigated catalysts.

Catalyst	BET surface area (m^2/g)
Al_2O_3	172
SA	163
0.1% Pd/Al_2O_3	165
0.1% Pd/SA	158

3. Results and discussion

3.1. BET surface area

Table 1 shows the BET surface areas of the four catalysts. A slightly decrease of the surface areas of γ-Al_2O_3 after sulfation and calcination was observed which may be explained by the coverage of the surface Al_2O_3 by sulfate ions [39]. The loading of Pd on the γ-Al_2O_3 and SA supports caused a slight decrease of the BET surface areas.

3.2. CO adsorption

The samples were evacuated at room temperature, then pretreated with oxygen at 500 °C for 30 min and followed by evacuation at the same temperature for 1 h. CO was introduced to Al_2O_3, Pd/Al_2O_3, SA and Pd/SA samples at −120 °C and the obtained IR spectra were shown in Fig. 1.

The adsorption of CO on the activated Al_2O_3 sample resulted in the appearance of a high intensity band positioned at 2196 cm^{-1}. This peak can be assigned to Al^{3+}–CO species [44]. When Pd

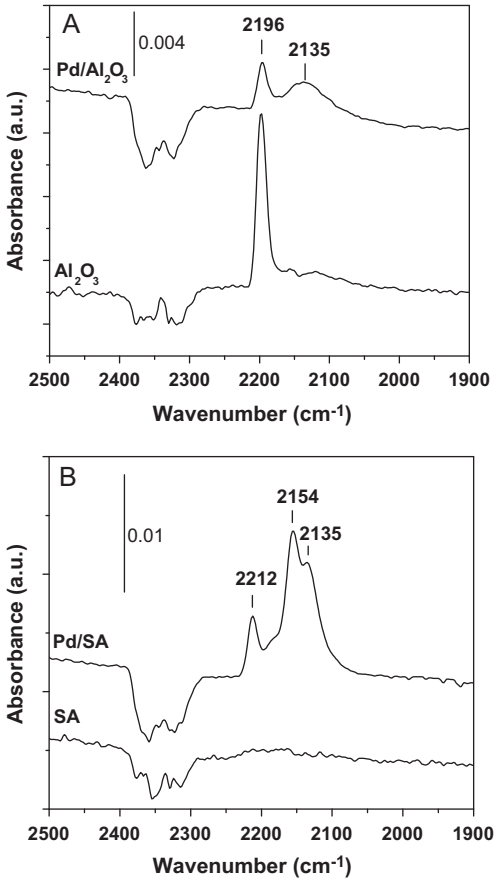

Fig. 1. IR spectra of adsorption of CO (5.00 Torr) on unsulfated catalysts Al_2O_3, Pd/Al_2O_3 (A), and sulfated catalysts SA, Pd/SA (B) at −120 °C for 40 min followed by brief evacuation.

supported on Al_2O_3 sample, the Al^{3+}–CO species decreased in intensity. At the same time, a new weaker band with the maximum at 2135 cm^{-1} appeared.

For SA sample, no CO adsorption was observed. This indicated that sulfation may change the surface and prevents the CO adsorption on Al_2O_3. For Pd/SA sample, there were three bands formed with the maximum peak at about 2212, 2154 and 2135 cm^{-1}.

According to the literatures [44–47], it was already noted that linear Pd^{2+}–CO species absorb in the region of 2215–2140 cm^{-1}, Pd^{+}–CO carbonyls at 2145–2100 cm^{-1}, and Pd^{0}–CO species below 2100 cm^{-1}. The Pd^{2+}–CO complexes are usually observed in a narrower range, namely at 2170–2145 cm^{-1}, while higher wavenumbers have been only reported with palladium in zeolites [48]. So in our case, the band at 2212 cm^{-1} can be assigned to Pd^{3+}–CO [48,49], the band at 2154 cm^{-1} may be assigned to the linear Pd^{2+}–CO and the band at 2135 cm^{-1} is due to the complexes of Pd^{2+}–CO species and Pd^{+}–CO carbonyls. We also notice that the intensities of the carbonyls bands formed on the Pd/SA sample are significantly higher than those formed on Pd/Al_2O_3. As reported on some similar systems (such as sulfated zirconia, tungstated zirconia, tungstated alumina) [27,28,38,41], the sulfation could generate strong BrØnsted acid which can stabilize Pd as highly dispersed Pd^{2+} ions on Pd/SA sample. While on Pd/Al_2O_3 sample, Pd mostly exists as PdO, which adsorbs CO weakly and is active for the complete oxidation of methane.

3.3. NO adsorption

Fig. 2 shows the IR spectra of NO adsorption over Al_2O_3, Pd/Al_2O_3, SA, and Pd/SA at room temperature for 40 min followed by evacuation for 30 min. The adsorption of NO on Al_2O_3 produces bands at 1656, 1461, 1318, 1228, and 1074 cm^{-1}. According to literature [50], the bands at 1461, 1318, 1228, and 1074 cm^{-1} can be attributed to nitro/nitrito species, which will disappear at excess of oxygen. While the band at 1656 cm^{-1} is due to bridging nitrates (ν_3'). NO adsorption on Pd/Al_2O_3 increases the intensities of these bands, implying loading of Pd promotes the adsorption of NO on Al_2O_3. When NO adsorbs on SA, a strong negative peak at 1404 cm^{-1} develops. At the same time, a broad and poorly resolved absorption band at 1296 cm^{-1} and a weak band at 1171 cm^{-1} in the region of 1400–1100 cm^{-1} appear. These species (1404, 1296, 1171 cm^{-1}) are due to sulfate groups perturbed by water [51]. In the higher frequency region, two new bands at 1629 and 1680 cm^{-1} appear. These peaks can be respectively assigned to the adsorbed water and the *cis*-HNO_2 formed by disproportionation of NO with participation of the OH groups on the SA surface according to the following reaction (1) [42,51]. This process should lead also to the formation of NO^- species. However, no absorption that can be assigned to an anionic nitrosyl, NO^-, is observed. It can be proposed that NO^- species are oxidized fast by sulfated ions (for example, to NO_3^- and NO_2^-) according to the reactions (2) and (3) [51]. Because the *cis*-HNO_2 and adsorbed water bands cover the region from 1700 to 1500 cm^{-1}, we cannot observe the bands of NO_3^- species at the wavenumber higher than 1500 cm^{-1}. Likewise, due to the overlapping with the perturbed sulfate groups, we cannot observe the peaks of NO_2^- species which should appear at 1400–1000 cm^{-1} either [52]. This behavior is similar to what was observed on SZ [51].

$$2NO + OH^- \rightarrow HNO_2 + NO^- \rightarrow NO^- + NO_2^- + H_2O \quad (1)$$

$$NO^- + 2SO_4^{2-} \rightarrow NO_3^- + 2SO_3^{2-} \quad (2)$$

$$NO^- + SO_4^{2-} \rightarrow NO_2^- + SO_3^{2-} \quad (3)$$

Comparing the spectrum of NO adsorption on SA with that on Pd/SA, we can see that the loading of Pd leads to an increase in the intensities of absorption bands. With the enhancement in the intensity of the negative peak, the positive bands at 1296 and 1171 cm^{-1} also increase. This further confirms that the peaks at 1296 and 1171 cm^{-1} come from the SO_4^{2-} group perturbed by water formed as a result of the interaction between NO and surface hydroxyls [42]. This interaction can also be proved by the decrease in the intensity of isolated hydroxyl groups with bands at 3788, 3716 cm^{-1} and the appearance of a broad band at 3464 cm^{-1} assignable to H-bonded hydroxyls with prolonging contact of NO over Pd/SA sample [50] (see Fig. 3).

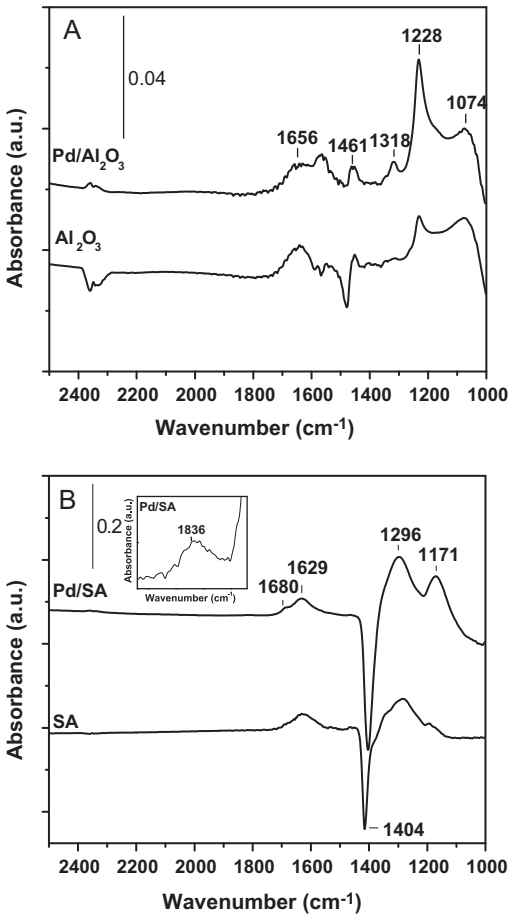

Fig. 2. IR spectra of adsorption of NO (3.00 Torr) on unsulfated catalysts Al_2O_3, Pd/Al_2O_3 (A), and sulfated catalysts SA, Pd/SA (B) evacuated at room temperature for 40 min followed by evacuation for 30 min.

According to the analyses of the spectra of NO adsorption on the four different samples, we can conclude that Pd facilitates NO adsorption, both on Al_2O_3 and on SA. This result is further proved by the NO-TPD results on SA and Pd/SA. Comparing the intensities of NO desorption on SA with that on Pd/SA in Fig. 4, we can conclude that Pd obviously increase the NO adsorption on SA catalyst.

3.4. NO–O_2 co-adsorption

3.4.1. NO–O_2 co-adsorption at room temperature

Fig. 5 displays the IR spectra of Al_2O_3, Pd/Al_2O_3, SA, and Pd/SA after co-adsorption of NO and O_2. Both Al_2O_3 and Pd/Al_2O_3 yield bands at 1619, 1585, and 1564 cm^{-1} when co-adsorption of NO and O_2. These bands can be attributed to bridged, bidentate and monodentate nitrates, respectively [50,53–55]. The structures of the three kinds of nitrates are shown in Table 2. In addition, a strong band at 1305 cm^{-1} develops and its assignment will be discussed in the following part. In the ν(OH)-stretching region, negative bands

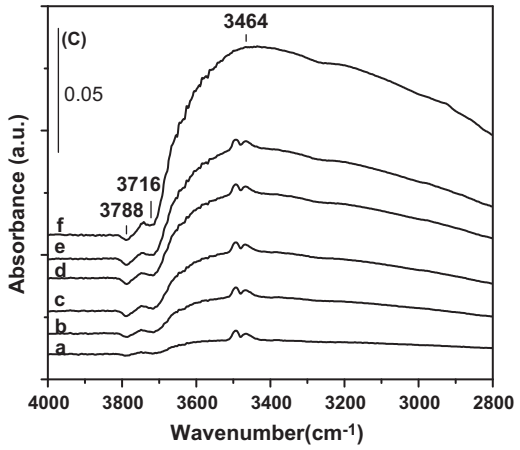

Fig. 3. IR spectra of adsorption of NO (3.00 Torr) on Pd/SA catalyst at room temperature in the O–H stretching region for 1 min (a), 10 min (b), 20 min (c), 30 min (d), and 40 min (e), followed by evacuation for 30 min (f).

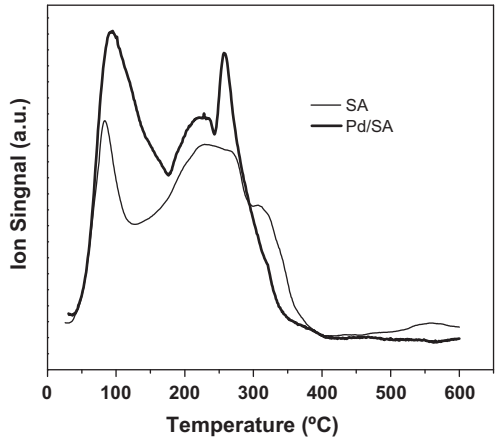

Fig. 4. NO-TPD profiles of SA and Pd/SA catalysts.

at 3753 and 3683 cm^{-1} as the characteristic of isolated hydroxyl groups are observed. At the same time, we also observed a positive broad band with its maximum at 3494 cm^{-1} assignable to H-bonded hydroxyls [50]. The very similar spectra of Al_2O_3 and Pd/Al_2O_3 suggest that the nitrate species are formed on the support rather than on Pd.

When NO and O_2 co-adsorbs on SA and Pd/SA samples, the bands corresponding to various coordinated nitrate species are observed at 1632, 1588 and 1564 cm^{-1}. For Pd/SA sample, a weak band at 1836 cm^{-1} is also observed. This species should be associated with the isolated Pd^{2+} ions, and was also observed when NO adsorbed on Pd/SA. The assignment of this band is still in debate: Pd^{2+}–NO, $Pd^{2+}(X)NO$ [$X = H_2O, NO_2$] or $H^+[Pd(OH)(NO)]^+$ were all proposed in the literature [27,35,37,56–59]. Among them, the latter two species require the Pd^{2+} ions possessing two coordination vacancies. To decide whether such Pd sites are available on the surface of our Pd/SA catalyst, we conducted DRIFTS experiment for the adsorption of CO according to the work of Bell and co-workers [49]. However,

Table 2
Nitrate species structure sketch model.

Bridged nitrate	Bidendate nitrate	Monodentate nitrate
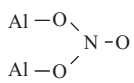	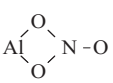	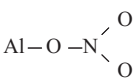

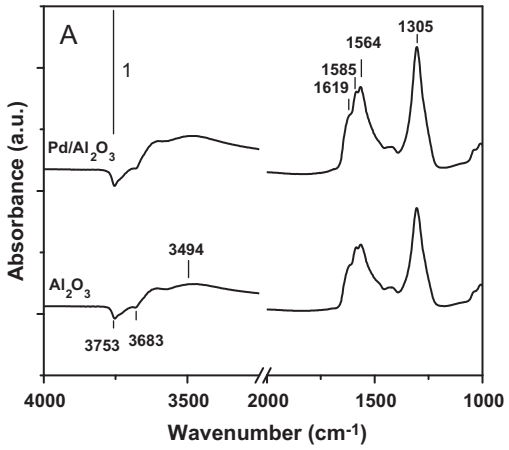

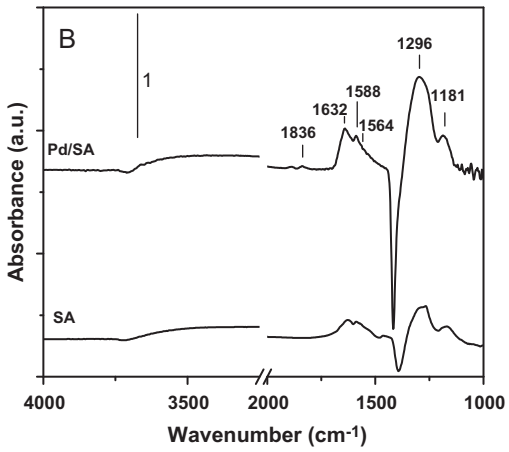

Fig. 5. IR spectra of co-adsorption of NO (3.00 Torr) and O_2 (6.00 Torr) on unsulfated catalysts Al_2O_3, Pd/Al_2O_3 (A), and sulfated catalysts SA, Pd/SA (B) at room temperature for 40 min followed by evacuation for 30 min.

the result (not shown here) indicates the Pd^{2+} sites on the SA support have not two coordination vacancies. Thereby, we attribute the band at 1836 cm^{-1} to Pd^{2+}–NO. Compared with absorption bands on the non-sulfated samples, the intensities of the absorption bands on the SA and Pd/SA samples decrease greatly, suggesting the sulfation of the support prevents the formation of the nitrate species to some extent. It is also found that on the sulfated samples the band intensity distribution of bridged, bidentate and monodentate nitrates are quite different from that on the non-sulfated samples. These results also approve that sulfation can change the surface property of support. The band at 1305 cm^{-1} observed on the non-sulfated samples disappears in the case of sulfated samples. In the high frequency region, the negative bands corresponding to stretching of hydroxyl groups become much weaker due to a portion of –OH groups displaced by SO_4^{2-} groups during the sulfation process [51].

3.4.2. Stability of nitrate species on different samples

As indicated above, there are three types of nitrate species formed by co-adsorption of NO and O_2 on the four samples. In order to study the reactivity of various nitrate species, we firstly investigated the thermal stabilities of these species under different temperatures. With an increase of the evacuation temperature, the nitrate species on the Al_2O_3 sample with absorption bands at 1619, 1585, and 1564 cm^{-1} decrease gradually in their intensities (Fig. 6A). At the same time, the absorption band at 1305 cm^{-1} evolves into two well-resolved bands at 1305 cm^{-1} and 1253 cm^{-1}. These bands can be assigned to mono- and bidentate nitrates and

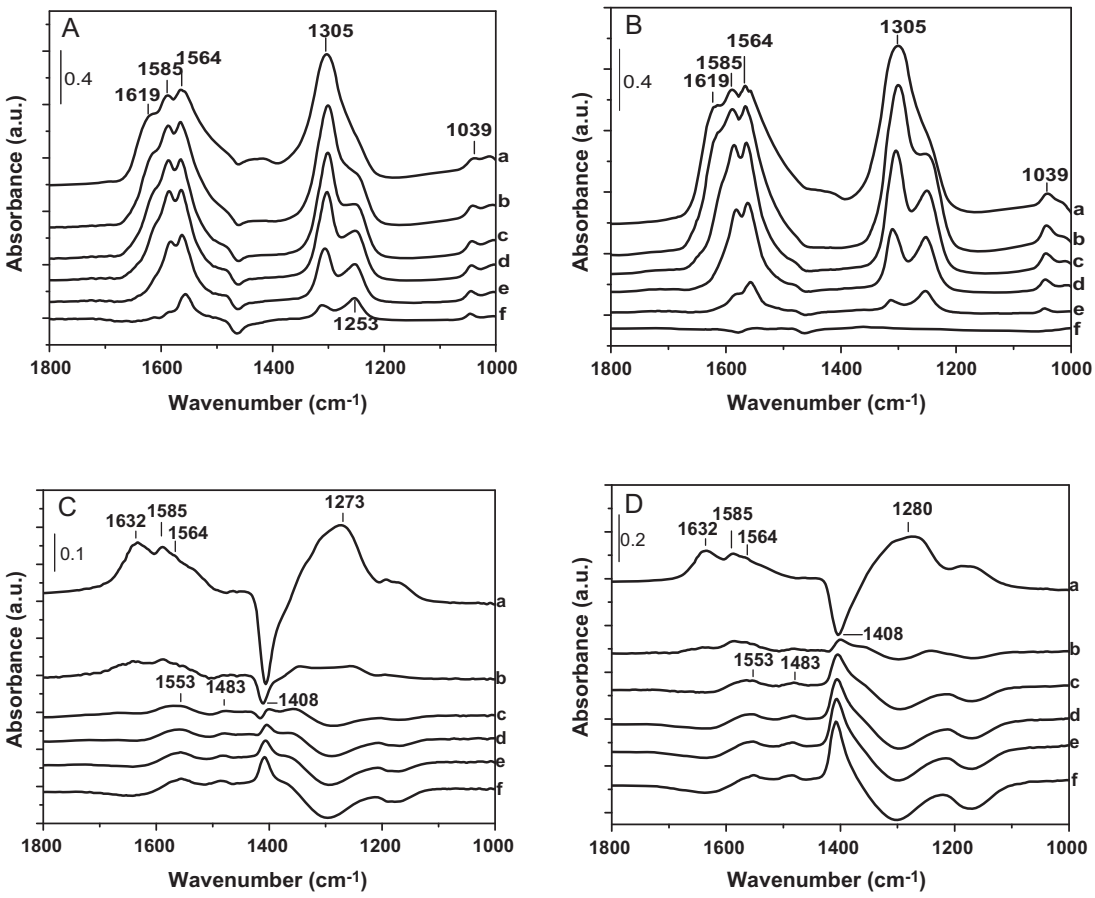

Fig. 6. Stability of surface NO_x compounds formed by co-adsorption of NO and O_2 on Al_2O_3 (A), Pd/Al_2O_3 (B), SA (C) and Pd/SA (D): evacuation for 30 min at room temperature (a) and at 250 °C (b), 350 °C (c), 400 °C (d), 450 °C (e), 500 °C (f).

bridged nitrates, respectively [50,54]. This result indicates that the thermal stabilities of different nitrate species on the Al_2O_3 sample are different. The Pd/Al_2O_3 sample displays a similar behavior with regard to the thermal stability of various nitrate species (Fig. 6B). However, it seems that the nitrate species on the Pd/Al_2O_3 sample are even less stable than those on Al_2O_3, as indicated by the complete disappearance of all the nitrate species on the Pd/Al_2O_3 sample when evacuation at 500 °C. This result implies that Pd promotes the decomposition of nitrate species.

In contrast to the non-sulfated samples, the two sulfated samples, either SA or Pd/SA (Fig. 6C and D), display weakly adsorption towards nitrate species. The nitrate species at 1564, 1585, and 1632 cm^{-1} disappear completely after evacuation at 350 °C. Concomitantly, two bands appeared at 1553 and 1483 cm^{-1}, which became more evident with the increase of evacuation temperature. According to the references [37,51], these two bands can be assigned to bidentate and monodentate nitrates. As a result of decreasing intensity of the absorption band at 1632 cm^{-1} with an increase of the evacuation temperature, a negative peak can even be observed at high temperatures. In addition, we noticed that the intensity of the negative band at 1408 cm^{-1} decrease with evacuation temperature indicating the restoration of the perturbed sulfated groups. This result suggests that the absorption band at 1632 cm^{-1} may also include H-bonded hydroxyls, i.e. water [43], which can overlap the surface nitrates (with bands at 1553 and 1483 cm^{-1}) at room temperature. Therefore, it could be inferred that the nitrate species with bands at 1553 and 1483 cm^{-1} most likely appear during $NO–O_2$ co-adsorption at room temperature. They can only be observed upon evacuation at high temperatures or after the desorbing of H-bonded hydroxyls.

3.5. Interaction of the intermediates with methane and/or oxygen

3.5.1. Reactivity of the nitrate species formed on sulfated samples towards methane

Fig. 7 displays the IR spectra obtained in the reaction between the nitrate species formed over sulfated samples with bands at 1553 and 1483 cm^{-1} and methane. To do that, SA or Pd/SA samples was exposed to NO and O_2 for 40 min at room temperature followed by evacuation at room temperature and 350 °C for 30 min, respectively. After cooling to room temperature (Fig. 7, spectrum a), methane was added. Then, the closed IR cell was heated from room temperature to 350 °C (Fig. 7, spectrum b), 400 °C (Fig. 7, spectrum c), 450 °C (Fig. 7, spectrum d), and 500 °C (Fig. 7, spectrum e), and kept at each temperature for 40 min. For the SA sample, introduction of CH_4 did not cause any changes of nitrate species at 1553 and 1483 cm^{-1}, even by further increasing the temperature up to 500 °C (Fig. 7A). At the same time, no CO_2 was produced. This result indicates that the nitrate species on the SA sample cannot react with CH_4.

On the contrary, significant changes took place on the Pd/SA sample after introduction of CH_4. As shown in Fig. 7B, when CH_4 was introduced to the sample at 350 °C, a slight decrease in intensities of bands at 1553 and 1483 cm^{-1} can be observed. With the elevation of the reaction temperature, the nitrate species decrease more clearly and almost disappear at 450 °C. When the temperature is up to 500 °C these species disappear completely. A broad peak characteristic of adsorbed water appears at 1628 cm^{-1} [43] and the intensity of CO_2 observed at 2348 cm^{-1} obviously increases with the temperature elevation. This result strongly suggests that the nitrate species on Pd/SA react with CH_4 to produce N_2, CO_2 and

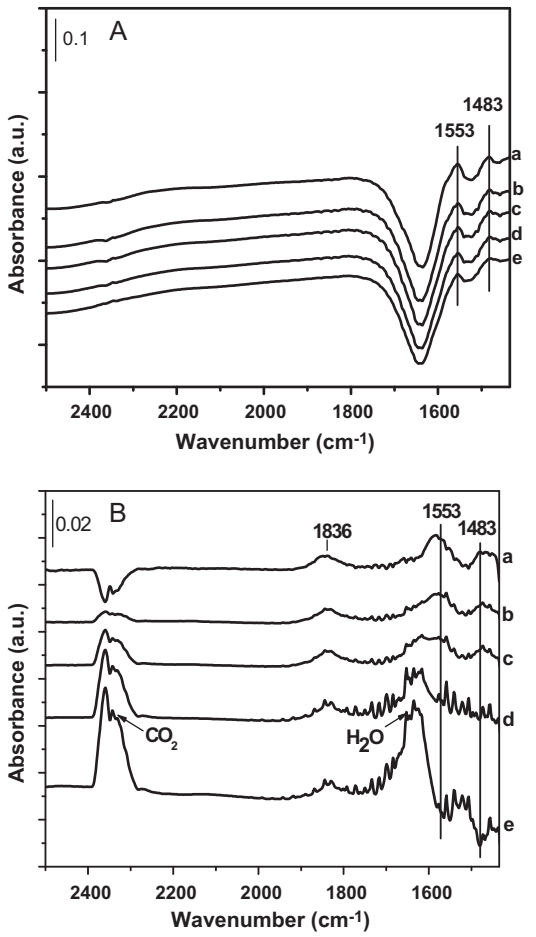

Fig. 7. IR spectra of co-adsorption of NO and O_2 over SA (A) and Pd/SA (B) at room temperature followed by evacuation at 350 °C (a), introduction of 1%CH_4/He (16.00 Torr) at room temperature, and then elevated the temperature to 350 °C (b), 400 °C (c), 450 °C (d), 500 °C (e).

H_2O. The optimum reaction temperature is in well agreement with our activity testing result [39].

Since the nitrate species at 1553 and 1483 cm^{-1} observed on the sulfated samples can react with CH_4 only in the presence of Pd which mainly exists as Pd^{2+} ions. The possible reaction route can be depicted as route 1 where the nitrate species act as the intermediates for the NO reduction with CH_4.

$$\text{Route 1}: \ NO + O_2 \xrightarrow{H^+} NO_3^- \xrightarrow[CH_4]{Pd^{2+}} N_2, CO_2, H_2O$$

At the same time, we noticed that the Pd^{2+}–NO species with a broader absorption band at 1836 cm^{-1} was almost unchanged with the temperature in CH_4 atmosphere. Therefore, we could conclude that this species hardly react with methane.

3.5.2. The surface reaction between Pd^{2+}–NO and methane and/or oxygen

Fig. 8 shows the spectra obtained from the in situ DRIFTS test over Pd/SA sample at 350 °C. Introducing NO and O_2 to the Pd/SA sample led to the generation of Pd^{2+}–NO species (spectrum a). In addition, a broad band at 1400 cm^{-1} assigned to sulfate groups was also observed [51]. Then CH_4 was introduced to the system, and the intensity of Pd^{2+}–NO species was found to be unchanged. However, upon introduction of O_2 to this system, the intensity of the Pd^{2+}–NO species decreased obviously, and disappeared with extending of reaction time. This result implies that O_2 is necessary for the reduction of NO with methane. According to literature [40],

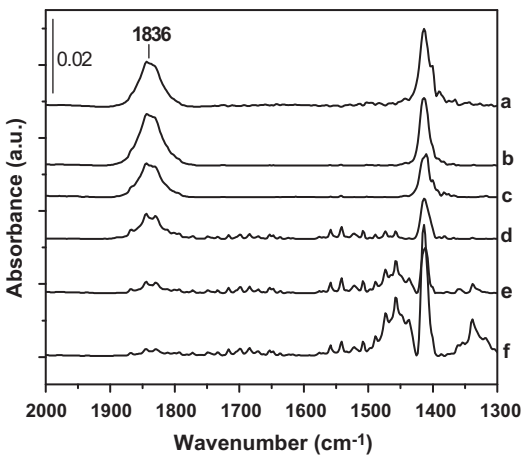

Fig. 8. DRIFTS spectra of adsorbed species on Pd/SA at 350 °C in flowing (a) NO + O_2 for 30 min, (b) CH_4 for 30 min, (c) CH_4 + O_2 for 1 min, (d) CH_4 + O_2 for 10 min, (e) CH_4 + O_2 for 20 min, (f) CH_4 + O_2 for 30 min. The feed gas compositions are as follows: 2000 ppm NO, 2000 ppm CH_4, 2% O_2, and the balance of He.

methane may be partially oxidized to formate over the Lewis acid sites on Pd/SA catalyst, and then these formate species react with Pd^{2+}–NO to produce N_2, CO_2 and H_2O.

The results are consistent with that in Fig. 7B, namely the Pd^{2+}–NO species produced on Pd/SA sample at the temperatures higher than 350 °C is an intermediate, and it could readily react with CH_4 and O_2, but not react with CH_4 in the absence of O_2. According to the results above, we propose the following reaction route of SCR of NO with methane over Pd/SA catalyst:

$$\text{Route 2}: \ NO + O_2 \underset{\text{over 350°C}}{\xrightarrow{Pd^{2+},H^+}} Pd^{2+} - NO \xrightarrow{CH_4,O_2} N_2, CO_2, H_2O$$

4. Conclusions

In this work, we investigated the SCR of NO with CH_4 over Pd/SA catalyst with FT-IR and DRIFTS. It was found that the sulfation of support can stabilize Pd as isolated Pd^{2+} ions. The introduction of Pd promotes the formation of nitro/nitrito and nitrate species on Al_2O_3 or SA at room temperature. Sulfation decreases the total concentration and thermal stability of the nitrates adsorbed on the surface of catalysts. The nitrate species observed over sulfated samples after evacuation at high temperatures can react with methane in the presence of Pd^{2+} to produce N_2, H_2O and CO_2.

In addition, for the co-adsorption of NO and O_2 on Pd/SA sample, we can observe Pd^{2+}–NO with absorption band at 1836 cm^{-1}. The Pd^{2+}–NO could readily react with CH_4 over 350 °C under the presence of O_2, but almost no reaction in the absence of O_2. This result indicates that the partial oxidation/or activation of methane is also necessary for the reduction of NO.

Acknowledgment

Financial support was provided by the National Science Foundation of China (NSFC) grants (20773122, 20773124, 20803079)

References

[1] M. Iwamoto, H. Yahiro, Y. Yu-u, S. Shundo, N. Mizuno, Shokubai (Japanese) 32 (1990) 430–433.
[2] M. Iwamoto, H. Yahiro, Catal. Today 22 (1994) 5–18.
[3] H. Hamada, Catal. Today 22 (1994) 21–40.
[4] M. Iwamoto, Catal. Today 29 (1996) 29–35.
[5] J.W. Tang, T. Zhang, D.B. Liang, C.H. Xu, X.Y. Sun, L.W. Lin, J. Chem. Soc., Chem. Commun. 19 (2000) 1861–1862.
[6] M.D. Fokema, J.Y. Ying, Catal. Rev. Sci. Eng. 43 (2001) 1–29.

[7] A.Q. Wang, D.B. Liang, C.H. Xu, X.Y. Sun, T. Zhang, Appl. Catal. B 32 (2001) 205–212.
[8] R. Burch, Catal. Rev. Sci. Eng. 46 (2004) 271–334.
[9] L.L. Ren, T. Zhang, D.B. Liang, C.H. Xu, J.W. Tang, L.W. Lin, Appl. Catal. B 35 (2002) 317–321.
[10] J.N. Armor, Catal. Today 26 (1995) 147–158.
[11] Y.J. Li, J.N. Armor, Appl. Catal. B 1 (1992) L31–L40.
[12] M.C. Campa, D. Pietrogiacomi, S. Tuti, G. Ferraris, V. Indovina, Appl. Catal. B 18 (1998) 151–162.
[13] Q. Sun, W.M.H. Sachtler, Appl. Catal. B 42 (2003) 393–401.
[14] J.W. Tang, T. Zhang, L. Ma, L. Li, J.F. Zhao, M.Y. Zheng, L.W. Lin, Catal. Lett. 73 (2001) 193–197.
[15] K. Yogo, E. Kikuchi, Stud. Surf. Sci. Catal. 84 (1994) 1547–1554.
[16] X.J. Zhou, Z.S. Xu, T. Zhang, L.W. Lin, J. Mol. Catal. A 122 (1997) 125–129.
[17] X.D. Wang, T. Zhang, C.H. Xu, X.Y. Sun, D.B. Liang, L.W. Lin, J. Chem. Soc., Chem. Commun. 4 (2000) 279–280.
[18] L.L. Ren, T. Zhang, J.W. Tang, J.F. Zhao, N. Li, L.W. Lin, Appl. Catal. B 41 (2003) 129–136.
[19] Y.J. Li, J.N. Armor, J. Catal. 145 (1994) 1–9.
[20] C.J. Loughran, D.E. Resasco, Appl. Catal. B 7 (1995) 113–126.
[21] D. Pietrogiacomi, S. Tuti, M.C. Campa, V. Indovina, Appl. Catal. B 28 (2000) 43–54.
[22] D. Pietrogiacomi, M.C. Campa, S. Tuti, V. Indovina, Appl. Catal. B 41 (2003) 301–312.
[23] N. Li, A.Q. Wang, J.W. Tang, X.D. Wang, D.B. Liang, T. Zhang, Appl. Catal. B 43 (2003) 195–201.
[24] T. Maunula, Y. Kintaichi, M. Inaba, M. Haneda, K. Sato, H. Hamada, Appl. Catal. B 15 (1998) 291–304.
[25] N. Li, A.Q. Wang, X.D. Wang, M.Y. Zheng, R.H. Cheng, T. Zhang, Appl. Catal. B 48 (2004) 259–265.
[26] A. Ali, W. Alvarez, C.J. Loughran, D.E. Resasco, Appl. Catal. B 14 (1997) 13–22.
[27] Y.H. Chin, W.E. Alvarez, D.E. Resasco, Catal. Today 62 (2000) 159–165.
[28] Y.H. Chin, A. Pisanu, L. Serventi, W.E. Alvarez, D.E. Resasco, Catal. Today 54 (1999) 419–429.
[29] D.K. Captain, K.L. Roberts, M.D. Amiridis, Catal. Today 42 (1998) 93–100.
[30] M. Shelef, Chem. Rev. 95 (1995) 209–225.
[31] S. Matsumoto, Catal. Today 29 (1996) 43–45.
[32] D. Yang, J.H. Li, M.F. Wen, C.L. Song, Catal. Lett. 122 (2008) 138–143.
[33] L.F. Córdoba, W.M.H. Sachtler, C.M. De Correa, Appl. Catal. B 56 (2005) 269–277.
[34] C.E. Quincoces, S. Guerrero, P. Araya, M.G. González, Catal. Commun. 6 (2005) 75–80.
[35] M. Kantcheva, I. Cayirtepe, Catal. Lett. 115 (2007) 148–162.
[36] Y.H. Chin, W.E. Alvarez, D.E. Resasco, Catal. Today 62 (2000) 291–302.
[37] M. Kantcheva, I. Cayirtepe, J. Mol. Catal. A 247 (2006) 88–98.
[38] K. Okumura, T. Kusakabe, M. Niwa, Appl. Catal. B 41 (2003) 137–142.
[39] N. Li, A.Q. Wang, L. Li, X.D. Wang, L.L. Ren, T. Zhang, Appl. Catal. B 50 (2004) 1–7.
[40] S.C. Xu, J.H. Li, D. Yang, J.M. Hao, J. Phys. Chem. C 112 (2008) 16052–16059.
[41] R. Yoshimoto, K. Okumura, M. Niwa, Catal. Today 84 (2003) 159–164.
[42] M. Kantcheva, A.S. Vakkasoglu, J. Catal. 223 (2004) 352–363.
[43] M. Kantcheva, A.S. Vakkasoglu, J. Catal. 223 (2004) 364–371.
[44] D. Tessier, A. Rakai, F. Bozon-Verduraz, J. Chem. Soc. Faraday Trans. 88 (1992) 741–749.
[45] D. Amalric-Popescu, F. Bozon-Verduraz, Catal. Lett. 64 (2000) 125–128.
[46] W. Juszczyk, Z. Karpiński, I. Ratajczykowa, Z. Stanasiuk, J. Zieliński, L.-L. Shen, W.M.H. Sachtler, J. Catal. 120 (1989) 68–77.
[47] K.I. Hadjiivanov, G.N. Vayssilov, Adv. Catal. 47 (2002) 307–511.
[48] P. Vijayanand, K. Chakarova, K. Hadjiivanov, P. Lukinskas, H. Knözinger, Phys. Chem. Chem. Phys. 5 (2003) 4040–4044.
[49] W. Aylor, L.J. Lobree, J.A. Reimer, A.T. Bell, J. Catal. 172 (1997) 453–462.
[50] T. Venkov, K.I. Hadjiivanov, D. Klissurski, Phys. Chem. Chem. Phys. 4 (2002) 2443–2448.
[51] M. Kantcheva, E.Z. Ciftlikli, J. Phys. Chem. B 106 (2002) 3941–3949.
[52] S.J. Huang, A.B. Walters, M.A. Vannice, J. Catal. 192 (2000) 29–47.
[53] Ch. Sedlmair, K. Seshan, A. Jentys, J.A. Lercher, J. Catal. 214 (2003) 308–316.
[54] B. Westberger, E. Fridell, J. Mol. Catal. A 165 (2001) 249–263.
[55] A. Desikusumastuti, T. Staudt, H. Grönbeck, J. Libuda, J. Catal. 255 (2008) 127–133.
[56] C. Descorme, P. Gé1in, M. Primet, C. Lécuyer, Catal. Lett. 41 (1996) 133–138.
[57] L.J. Lobree, A.W. Aylor, J.A. Reimer, A.T. Bell, J. Catal. 181 (1999) 189–204.
[58] E.M. Holmgreen, M.M. Yung, U.S. Ozkan, J. Mol. Catal. A 270 (2007) 101–111.
[59] C. Descorme, P. Gélin, C. Lécuyer, M. Primet, J. Catal. 177 (1998) 352–362.